Formation and Decay of the S3 EPR Signal Species in Acetate-Inhibited Photosystem II†

Veronika A. Szalai and Gary W. Brudvig*

Department of Chemistry, Yale University, New Haven, Connecticut 06511

Received October 4, 1995; Revised Manuscript Received November 27, 1995⊗

ABSTRACT: A 230-G-wide EPR signal is induced in acetate-treated photosystem II by 30 s of illumination at 277 K followed by freezing under illumination to 77 K [MacLachlan, D. J., & Nugent, J. H. A. (1993) *Biochemistry 32*, 9772−9780]. This signal, referred to as the S3 EPR signal, has been interpreted to arise from an S_2X^+ species where X^+ is an amino acid radical. Investigation of the factors responsible for the formation and decay of the S3 EPR signal reveals that the yield of the S3 EPR signal is strongly temperature-dependent and depends on the rate of oxidation of Q_A^-. Quantitation of the number of centers contributing to the S3 EPR signal produced by the optimal continuous illumination times of 3 min at 250 K, 30 s at 273 K, and 5 s at 294 K gave values of 13, 38, and 49 ± 3%, respectively. By using 5 s of illumination at 294 K to induce the S3 EPR signal, and then illumination at 200 K to reduce Q_A, both the S3 and Q_A^-Fe EPR signals were induced in high yield. This result indicates that the S3 EPR signal does not arise from an acceptor-side species. When saturating laser flashes were used to induce the S3 EPR signal in a dark-prepared, dark-adapted, acetate-treated sample, the yield was small after one flash and close to maximal after two flashes. An EPR signal at $g = 4.1$ was observed to be formed at intermediate times during the decay of the S3 EPR signal in the dark; the rates of decay of the S3 EPR signal at 273 and 294 K corresponded to the rates of formation of the $g = 4.1$ EPR signal. These results, together with the flash results, indicate that two steps are involved in both the generation and decay of the S3 EPR signal. The rates of formation and decay of both the S3 and Q_A^-Fe EPR signals were measured at 250, 273, and 294 K. A kinetic model is presented that accounts for these kinetic data and the yield of the S3 EPR signal.

Photosystem II (PSII)[1] catalyzes the light-driven oxidation of water to dioxygen and reduction of plastoquinone to plastoquinol in plant photosynthesis (Ghanotakis & Yocum, 1990; Rutherford et al., 1992). Four photons of light must be absorbed, and the OEC, a tetranuclear manganese cluster of unknown structure (Debus, 1992), must be oxidized 4 times in order for dioxygen to be produced. Each successive oxidation of the OEC has been termed a "store" or S state (Kok et al., 1970). Therefore, the OEC cycles through five states labeled S_0 to S_4 with O_2 being evolved between the S_4 and S_0 states. The oxidations associated with each S-state advance may be exclusively attributed to oxidation of the Mn_4 cluster (Dekker et al., 1984; Ono et al., 1992) or to oxidations involving both the Mn_4 cluster and a neighboring amino acid residue (Boussac et al., 1989, 1990b; Guiles et al., 1990; Nugent et al., 1993).

In untreated, dark-adapted PSII, the OEC is primarily in the diamagnetic S_1 resting state (Beck et al., 1985; Koulougliotis et al., 1992). By continuous illumination at 200 K, the OEC can be photooxidized to the S_2 state in high yield (Brudvig et al., 1983). The S_2 state displays a characteristic multiline EPR spectrum (Dismukes & Siderer, 1980) attributed to an $S = {}^1/_2$ ground state of an exchange-coupled manganese tetramer. Another EPR signal at $g = 4.1$ arising from another conformer of the S_2 state has been proposed to arise from an $S = {}^3/_2$ or $S = {}^5/_2$ state (dePaula et al., 1987; Haddy et al., 1992).

In PSII which has been subjected to various inhibitory treatments including calcium or chloride depletion, the properties of the S_2 and S_3 states are altered, and the water-oxidation chemistry is blocked. Calcium depletion and chloride depletion directly affect the donor side of PSII by removing tightly bound calcium (Boussac & Rutherford, 1988) or chloride (Itoh et al., 1984; Theg et al., 1984; Sinclair, 1984; Damoder et al., 1986; Saygin et al., 1986) from a site near the OEC. A dark-stable form of the S_2-state multiline EPR signal has been observed in PSII which has been NaCl washed and treated with EGTA or EDTA or in citrate-washed PSII samples (Boussac et al., 1990a; Ono & Inoue, 1990). It exhibits more hyperfine peaks with smaller couplings than the S_2-state multiline EPR signal observed in untreated PSII (Boussac et al., 1989). A broad EPR signal centered at approximately $g = 2.0$, referred to as the S3 EPR signal, has also been observed in inhibited PSII upon continuous illumination at temperatures above 250 K (Boussac et al., 1989). The width (and sometimes structure) of the S3 EPR signal varies from approximately 100 G in ammonia-treated samples (Andréasson & Lindberg, 1992) to 160 G in calcium-depleted samples (Boussac et al.,

† This work was supported by the National Institutes of Health (GM32715).

⊗ Abstract published in *Advance ACS Abstracts*, January 15, 1996.

[1] Abbreviations: chl, chlorophyll; DMSO, dimethyl sulfoxide; EDTA, ethylenediaminetetraacetic acid; EGTA, ethylene glycol bis-(β-aminoethyl ether)-*N*,*N*,*N*′,*N*′-tetraacetic acid; EPR, electron paramagnetic resonance; FCCP, carbonyl cyanide *p*-(trifluoromethoxy)-phenylhydrazine; MES, 2-(*N*-morpholino)ethanesulfonic acid; OEC, O_2-evolving complex; PNPDU, 3-(phenylnitroxylphenyl)-1,1-dimethylurea; PPBQ, phenyl-*p*-benzoquinone; PSII, photosystem II; Q_A, tightly bound plastoquinone in PSII; Q_B, exchangeable plastoquinone in PSII; Tris, tris(hydroxymethyl)aminomethane; Y_D, tyrosine 161 of the D2 polypeptide; Y_Z, tyrosine 161 of the D1 polypeptide.

0006-2960/96/0435-1946$12.00/0

1989) to 230 G in acetate-treated samples (MacLachlan & Nugent, 1993). Based in part on flash experiments (Baumgarten et al., 1990; Boussac et al., 1990b), EPR spectroscopy (Boussac et al., 1989; Sivaraja et al., 1989; Baumgarten et al., 1990), and X-ray absorption studies of the S_2 to S_3 transition (Guiles et al., 1990; Nugent et al., 1993), the S3 EPR signal is proposed to arise from weak exchange coupling of the Mn_4 cluster with an organic radical in the configuration S_2X^+ (X^+ = organic radical). Assuming an initial dark state of S_1, two electrons need to be transferred from the donor side to give the final state S_2X^+. However, both the oxidation state of the manganese cluster and the identity of the organic radical are under debate (Baumgarten et al., 1990; Boussac & Rutherford, 1992; Boussac et al., 1992; Hallahan et al., 1992; MacLachlan & Nugent, 1993; Ono et al., 1994; Gilchrist et al., 1995).

In untreated PSII, selective two-electron oxidation of the OEC to the S_3 state in high yield in concentrated samples was not possible until recently. Our laboratory has used the redox-active herbicide PNPDU which binds tightly in place of plastoquinone in the Q_B site in order to use continuous illumination to produce the S_3 state in about 80% yield (Bocarsly & Brudvig, 1992). Because two turnovers of PSII are needed to generate the S3 EPR signal, we were interested in limiting PSII, subjected to inhibitory treatments, to two turnovers by using the redox-active herbicide PNPDU. Our expectation was that PNPDU treatment, coupled with one of the other inhibitory treatments (calcium or chloride depletion or acetate treatment), would produce a high yield of the S3 EPR signal. However, when acetate-treated PSII was incubated with PNPDU and continuously illuminated at 250 K, the S3 EPR signal was not formed in high yield (Szalai & Brudvig, 1995). The low yield of the S3 EPR signal in these samples can be attributed to the slow reduction rate of the redox-active herbicide and fast decay rate of the S3 EPR signal. This led to an investigation of the factors influencing the formation and decay of the S3 EPR signal. Acetate treatment was chosen for the present studies for two reasons. First, acetate can simply be added to an untreated sample to produce a sample that gives an S3 EPR signal when illuminated at 0 °C. It has been argued that the main donor-side effect of acetate treatment is displacement of chloride (Sinclair, 1984; MacLachlan & Nugent, 1993). Second, the acceptor-side effects of acetate are well-defined (Blubaugh & Govindjee, 1988) and cause the light-induced Q_A^-Fe EPR signal to be converted from a broad signal at $g \approx 1.9$ to a sharp signal at $g \approx 1.8$ due to the binding of acetate in place of bicarbonate at or near the non-heme Fe(II). This change facilitates quantitation of the number of reducing equivalents on the acceptor side.

Since the species giving rise to the S3 EPR signal is proposed to be an organic radical with spin $^1/_2$, we have quantitated the number of centers giving rise to the S3 EPR signal by comparing the integrated area of the S3 EPR signal to the integrated area of the EPR signal from $Y_D^\bullet$. We have also addressed the origin of the S3 EPR signal. Although the donor side has been assumed to be the source of the S3 EPR signal, an acceptor-side species has not been firmly ruled out. By optimizing the illumination conditions, the S3 EPR signal in acetate-treated PSII can be generated in approximately 50% of the centers. The simultaneous formation of a high yield of the Q_A^-Fe EPR signal indicates that the S3 EPR signal does not arise from an acceptor-side species. Saturating laser-flash experiments and measurements of the decay of the S3 EPR signal indicate that both the formation and decay of the S3 EPR signal are two-step processes proceeding through the S_2 state. A kinetic model is presented that accounts for the yield of the S3 EPR signal observed upon continuous illumination of acetate-treated PSII.

MATERIALS AND METHODS

MES was purchased from Sigma. Ethylene glycol, DMSO, and sucrose were purchased from Baker and used without further purification. Anhydrous sodium acetate was purchased from Fisher Chemical, and sodium chloride was purchased from Mallinckrodt.

PSII membranes were isolated from market spinach leaves following the procedure of Berthold et al. (1981) with the modifications of Beck et al. (1985). The membranes were stored at 77 K in resuspension buffer [15 mM NaCl, 20 mM MES, and 30% (v/v) ethylene glycol at pH 6.0] at chlorophyll concentrations of approximately 6−8 mg of chl/mL until use. Chlorophyll concentrations were measured according to the method of Arnon (1949) on a Perkin-Elmer Lambda 3b Series UV/VIS spectrophotometer. Typical O_2 evolution rates of 300−400 μmol of O_2 (mg of chl)$^{-1}$ h^{-1} for untreated PSII were measured by using a Clarke electrode as in Beck et al. (1985).

For acetate-treated samples, 0.6 mL of PSII (6−8 mg of chl/mL) was resuspended in 30 mL of acetate buffer containing 40 mM MES, 0.3 M sucrose, and 500 mM sodium acetate at pH 5.5, and pelleted by centrifugation at 40000*g* for 20 min. An increased yield of the S3 EPR signal was observed in samples washed twice in buffer containing acetate, probably because of residual Ca^{2+} and/or Cl^- in the sample after only one wash. Therefore, the resuspension and centrifugation steps were repeated, and the pellet was resuspended in acetate buffer to a final chlorophyll concentration of 5−8 mg of chl/mL. Samples incubated with various acetate concentrations ranging from 10 mM to 500 mM produced no S3 EPR signal at acetate concentrations below 200 mM (data not shown). To show binding was complete, samples were incubated with 500 mM acetate for time periods ranging from 30 min to 6 h. Under these conditions, there was no significant change in the intensity of the S3 EPR signal (data not shown). When PSII was washed with constant ionic strength buffers containing varying amounts of acetate and chloride, both the S3 EPR signal due to acetate treatment and a narrower S3 EPR signal similar to that produced by calcium depletion could be observed. MacLachlan et al. (1994) have recently reported similar results in ammonium chloride-treated PSII at pH >7.0. These results indicate that it is probably both the removal of Ca^{2+} and/or Cl^- by the washing process and the effect of bound acetate which cause the lesion on the donor side of PSII that allows generation of the S3 EPR signal.

After being transferred to EPR tubes, PPBQ (Aldrich, 25 mM stock solution in DMSO) was added to give a final concentration of 500 μM. The samples were incubated in the dark at 0 °C for 30−60 min and then were frozen to 77 K in the dark. Samples which did not contain acetate were resuspended in buffer containing 40 mM MES and 0.3 M sucrose at pH 5.5. In all other respects, they were treated

as the acetate-treated samples described above. Continuous illuminations were performed with a quartz halogen lamp (700 W/m^2).

Low-temperature EPR spectroscopic measurements were performed on a Varian E-line EPR spectrometer equipped with an Oxford Instruments ESR 900 liquid helium cryostat with the following conditions unless otherwise noted: microwave frequency, 9.28 GHz; microwave power, 5 mW; magnetic field modulation frequency, 100 kHz; magnetic field modulation amplitude, 20 G; temperature, 6 K. Matched samples for EPR spectroscopy were prepared with and without acetate, and the intensity of the rhombic iron EPR signal at $g = 4.3$ was used for scaling spectra. The S3 EPR signal was produced by continuous illumination for 3 min at 250 K (dry ice/carbon tetrachloride slurry), by continuous illumination for 30 s at 0 °C, or by continuous illumination for 5 s at room temperature (294 K) followed by freezing in the dark to 77 K. The intensity of the S3 EPR signal was estimated as the peak height of the low-field ($g \approx 2.12$) component in light-minus-dark difference spectra unless otherwise noted. The S_2-state multiline EPR signal intensity was approximated as the sum of 4−8 hyperfine peak heights. The S_2-state $g = 4.1$ EPR signal peak-to-trough height was measured in light-minus-dark difference spectra. The maximum peak height of the sharp feature at $g \approx 1.8$ of the Q_A^-Fe EPR signal was measured by illuminating the sample for 5 min at 200 K (dry ice/ethanol slurry) following a 30−60 min dark adaptation at 0 °C.

The number of centers contributing to the S3 EPR signal was quantitated by collecting dark and light-induced spectra at three microwave powers. When the light-minus-dark difference spectra were integrated, the resultant spectra contained intensity from the S3 and $Y_D^\bullet$ EPR signals (see Figure 2); the total area of the light-minus-dark difference spectrum at each microwave power was measured. The percentage of the area from the S3 EPR signal was approximated by cutting out and weighing the portions which corresponded to the S3 and $Y_D^\bullet$ EPR signals. The yield of $Y_D^\bullet$ in acetate-treated PSII was compared to that in an untreated sample to determine whether $Y_D^\bullet$ was fully induced. EPR spectra of $Y_D^\bullet$ were collected for an acetate-treated PSII sample illuminated for 30 s at 0 °C or 7 min at 0 °C, an untreated sample of PSII in resuspension buffer [15 mM NaCl, 20 mM MES, 30% ethylene glycol (v/v), pH 7.5 (Buser & Brudvig, 1992)] illuminated for 30 s at 0 °C or 7 min at 0 °C, and an acetate-treated PSII sample illuminated for 3 min at 250 K. The yield of $Y_D^\bullet$ was the same in all five samples. In order to record the S3 EPR signal, it was necessary to use microwave powers that saturated the $Y_D^\bullet$ EPR signal. Power saturation data of $Y_D^\bullet$ were used to calculate the nonsaturated total area of the $Y_D^\bullet$ EPR signal at the microwave powers used to quantitate the S3 EPR signal (1, 2, and 5 mW). The area of the $Y_D^\bullet$ EPR signal obtained by this calculation represents one spin $^1/_2$ center per PSII. The numerical area of the S3 EPR signal was compared to the calculated area of the $Y_D^\bullet$ EPR signal to obtain the percentage of centers contributing to the S3 EPR signal. The percentages obtained from each of the microwave powers were averaged. It should be noted that these percentages are based on the assumption that the S3 EPR signal arises from a spin $^1/_2$ center.

For saturating-flash experiments, flashes were generated by a Candela SL 66 flash-lamp pumped dye laser with Rhodamine 590. The time between flashes was varied to determine the spacing between flashes which ensured that Q_A^- was fully reoxidized before the subsequent flash. From these experiments, the optimal interval between flashes was found to be 2.3 s. Samples were treated with PPBQ and dark-adapted for 6 h at 0 °C prior to acetate washing. All manipulations were done in the complete dark to avoid charge separation and possible S-state advancement. To determine the maximum PSII concentration that still allowed a saturating flash, single-flash experiments were performed at 0 °C. The Q_A^-Fe EPR signal was used as an internal standard to determine whether the flashes were saturating by comparing the intensity of the signal after a flash to the intensity induced by continuous illumination for 5 min at 200 K. These measurements indicated that saturating flashes could be achieved at chlorophyll concentrations at or below 1.5 mg/mL.

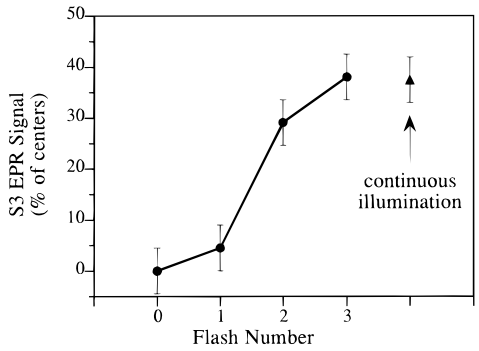

FIGURE 1: Plot of the percentage of PSII centers giving the S3 EPR signal versus flash number in acetate-treated PSII. In order to avoid overlapping signals, the intensity of the S3 EPR signal was measured at the high-field minimum in unsubtracted spectra. Saturating laser flashes were delivered at 0 °C and were spaced 2.3 s apart. [Chl] = 1.5 mg/mL.

RESULTS AND DISCUSSION

Saturating-Flash Experiments. Previous flash experiments on calcium-depleted EGTA-treated samples exhibiting the dark-stable S_2-state multiline EPR signal required only one flash to generate the S3 EPR signal; however, subsequent flashes to the same sample increased the yield of the S3 EPR signal (Boussac et al., 1990a). Flash experiments performed on dark-adapted fluoride-substituted PSII needed two flashes to produce some of the S3 EPR signal, but the intensity also increased upon the third and fourth flashes (Baumgarten et al., 1990). Because of the observation of some S3 EPR signal after only one (preilluminated sample) or two (dark-adapted sample) flashes, these results were interpreted in favor of the S_2X^+ assignment. The further increase in yield of the S3 EPR signal after more than two flashes may be due to a low quantum yield for its formation.

Figure 1 shows the results of saturating-flash experiments performed on acetate/PPBQ-treated samples. The S3 EPR signal after two flashes corresponds to almost the maximal intensity observed after three flashes or continuous illumination. These results indicate that the OEC must be oxidized by 2 equiv in order for the S3 EPR signal to be observed in acetate/PPBQ-treated samples and that the yield after two turnovers is close to the maximum. The high yield of the S3 EPR signal after just two flashes suggests that the quantum yield for formation of the S3 EPR signal in acetate-treated PSII may be higher than that found for calcium-

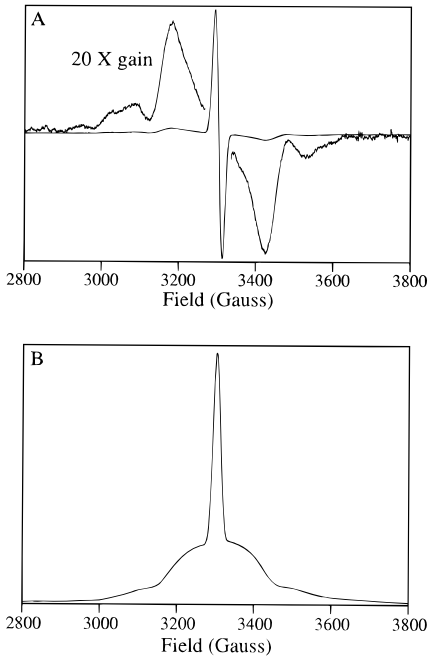

FIGURE 2: (A) Light-minus-dark difference spectrum of the S3 and $Y_D^\bullet$ EPR signals in acetate-treated PSII measured at 13 K. (B) Integrated spectrum of the light-minus-dark difference spectrum shown in (A). [Chl] = 6 mg/mL.

depleted or fluoride-substituted samples. However, the lower quantum yield observed in calcium-depleted and fluoride-substituted samples may have been due to a suboptimal spacing between flashes. In the case of calcium-depleted samples, a spacing of 1 s between flashes was used (Boussac & Rutherford, 1988; Boussac et al., 1990b). We found that approximately 2 s was required to reoxidize Q_A^-. The experiments on the fluoride-substituted samples used a spacing of 5 s between flashes (Baumgarten et al., 1990). This spacing could permit the S_2 state to decay before the second flash had been delivered and decrease the yield of the S3 EPR signal observed after the second flash.

Quantitation Results. Because the S3 EPR signal appears as a broadened feature at $g \approx 2.0$, it has been modeled as arising from a spin $^1/_2$ organic radical interacting with a fast relaxer such as the Mn_4 cluster (Boussac et al., 1990b; MacLachlan et al., 1994). If the S3 EPR signal arises from a spin $^1/_2$ system, the number of spins generating the signal can be quantitated by comparing the integrated area of the S3 EPR signal to a spin $^1/_2$ species of known concentration. When acetate-treated PSII is illuminated to produce the S3 EPR signal, $Y_D^\bullet$ is fully oxidized and provides a convenient spin $^1/_2$ internal standard. Figure 2B shows the integral of the light-minus-dark difference spectrum. The S3 EPR signal appears as shoulders on the central peak in Figure 2; the central sharp feature is due to $Y_D^\bullet$. By comparison of the integrated peak areas of the S3 EPR signal to the calculated area of $Y_D^\bullet$ (see Materials and Methods for details), the number of centers contributing to the S3 EPR signal was determined for different illumination conditions (Table 1). Five seconds of continuous illumination at room temperature (294 K) produced the S3 EPR signal in approximately 50% of the centers in acetate-treated PSII. The yields of the S3 EPR signal produced by 30 s of continuous illumination at 0 °C or 3 min of continuous illumination at 250 K were considerably smaller. Acceptor-side reactions in acetate-treated PSII are about 10-fold slower than in untreated PSII

Table 1: S3 EPR Signal Yield in Acetate-Treated PSII Produced by Continuous Illumination at Different Temperatures

temp (K)	continuous illumination time	yield of S3 EPR signal (% of PSII centers)
250	3 min	13 ± 3
273	30 s	38 ± 1
294	5 s	49 ± 3

(Saygin et al., 1986). If these reactions are rate-limiting, it could explain, in part, the temperature dependence of the yield of the S3 EPR signal. This explanation is considered in the Kinetics section.

Electron spin-echo experiments (Gilchrist et al., 1992) showed that fewer than 25% of the centers produced the S3 EPR signal in calcium-depleted PSII which had been continuously illuminated for 1 min at 0 °C. The yield of the S3 EPR signal in calcium-depleted PSII may also be sensitive to illumination time and temperature. When acetate-treated PSII was continuously illuminated at 0 °C for times ranging from 15 s to 3 min, the yield of the S3 EPR signal was found to be maximal at the shortest illumination time and then to decrease with further illumination (see Kinetics section). Since the amount of the S3 EPR signal produced by 1 min of continuous illumination at 0 °C was about half that produced by 30 s of continuous illumination at the same temperature (see Figure 4), the number of centers contributing to the S3 EPR signal after 1 min of illumination at 0 °C was approximately 20% in acetate-treated PSII. This figure is in good agreement with the results obtained by Gilchrist et al. (1992). Although possibly coincidental, the agreement may point to a similar lesion in the calcium-depleted and acetate-treated PSII samples as is also indicated by the observation of a calcium effect on the yield of the S3 EPR signal in acetate-treated PSII (MacLachlan & Nugent, 1993).

On the basis of these results, it would appear that the S3 EPR signal is not generated in the majority of the centers in inhibited PSII samples. One possibility is that the population of centers which produce the S3 EPR signal is damaged since the S3 EPR signal does not appear in untreated PSII and relatively harsh treatments (high ionic strength, low pH, or light incubation) are required to produce it. However, little S3 EPR signal is observed upon illumination of acetate-treated samples after calcium or chloride have been added [see Materials and Methods and MacLachlan and Nugent (1993)], which would argue that the centers producing the signal are not irreversibly damaged. Another possibility is that acetate treatment incompletely removes a tightly bound cofactor. Our observation that the S3 EPR signal yield does not increase after more than two washes with acetate-containing buffer or with prolonged treatment with acetate argues against this possibility. It is also possible that the S3 EPR signal does not arise from a donor-side species, but rather is from an acceptor-side radical. The S3 EPR signal could arise from the fraction of Q_A^- not observed as the Q_A^-Fe $g \approx 1.8$ EPR signal (see Acceptor Side vs Donor Side section). Finally, it is possible that the low yield of the S3 EPR signal is due to rapid decay of the radical species such that only a fractional amount is present in the steady-state produced by continuous illumination. This possibility is considered in the Kinetics section.

Acceptor Side vs Donor Side. When the S3 EPR signal was induced by 5 s of continuous illumination at room

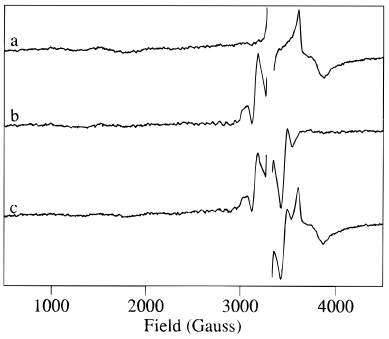

FIGURE 3: Comparison of the intensities of the S3 and Q_A^-Fe EPR signals in acetate-treated PSII induced by continuous illumination for (a) 5 min at 200 K, (b) 5 s at 294 K, or (c) 5 s at 294 K followed by 5 min at 200 K. Spectra are light-minus-dark difference spectra. [Chl] = 6 mg/mL.

temperature, the full amount of the sharp EPR signal due to Q_A^- coupled to the non-heme iron was not observed. These results, coupled with the quantitation results which show that the S3 EPR signal in acetate-treated samples does not arise from 100% of the centers, lead to the possibility that the S3 EPR signal could be arising from an acceptor-side species. Given this explanation, either a radical other than Q_A^- coupled to the non-heme iron or a change in the non-heme iron interaction with Q_A^- could be responsible for the S3 EPR signal.

To address this question, we consider the intensities of the Q_A^-Fe and S3 EPR signals. The S3 EPR signal generated by 5 s of continuous illumination at room temperature corresponded to about 50% of the centers (see Table 1). Under these illumination conditions, no Q_A^-Fe EPR signal was observed (Figure 3b). One way to resolve the question of whether the S3 EPR signal could arise from a fraction of Q_A not giving a Q_A^-Fe EPR signal is to find conditions where the number of centers producing the S3 EPR signal plus the number of centers producing an Q_A^-Fe EPR signal exceeds 100%. When acetate/PPBQ-treated samples were illuminated at room temperature to induce the S3 EPR signal and then illuminated at 200 K, both the Q_A^-Fe and S3 EPR signals were observed (Figure 3c). The Q_A^-Fe EPR signal was 80% of its maximum yield, and the S3 EPR signal accounted for approximately 40% of the centers. Because the combined yield was significantly greater than 100%, these experiments indicate that Q_A^- is not the species giving rise to the S3 EPR signal. Further, because the Q_A^-Fe EPR signal was identical with or without the S3 EPR signal present, these experiments also indicate that a radical other than Q_A^- interacting with the non-heme iron is not the species giving rise to the S3 EPR signal.

Formation and Decay Reactions. Because the S3 EPR signal was not observed in acetate-treated PSII containing the redox-active herbicide PNPDU (Szalai & Brudvig, 1995), we were led to believe that the rates of formation and decay of the S3 EPR signal play a significant role in determining its yield. Examination of the temperature dependence of the yields of the S3 EPR signal could clarify which processes are important in controlling the S3 yield and also give an indication of the origin of the S3 EPR signal. If an acceptor-side species such as Q_A^- were responsible for the S3 EPR signal, we would expect to see the yield of the S3 EPR signal decrease as the illumination temperature is increased because oxidation of the acceptor side by PPBQ is faster at higher

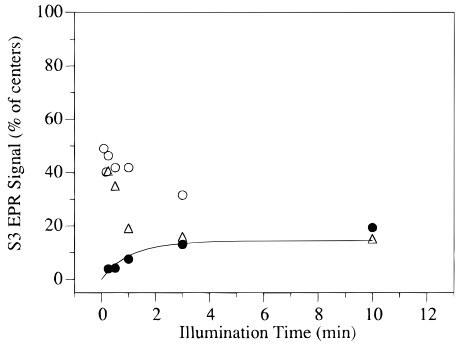

FIGURE 4: S3 EPR signal yield vs illumination time at (●) 250 K, (△) 273 K, and (○) 294 K. The calculated yield of the S3 EPR signal at 250 K (solid line) was determined by the kinetic model described in the text.

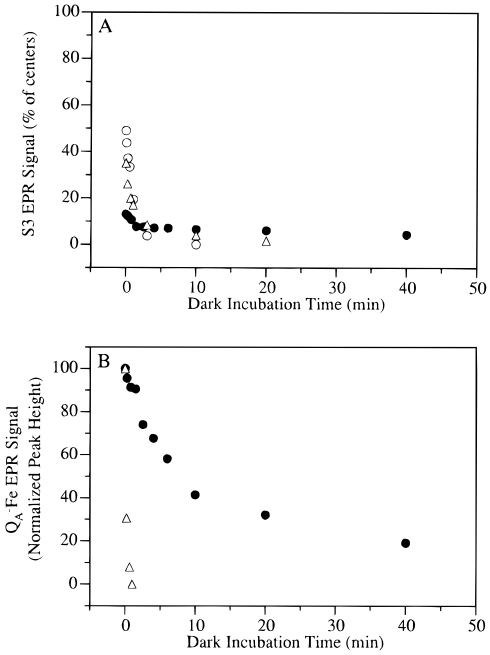

FIGURE 5: (A) Plot of the decays of the S3 EPR signal versus dark incubation time at (●) 250 K, (△) 273 K, and (○) 294 K. The S3 EPR signal intensities present after the illumination times given in Table 1 were used for the zero-time points. Data taken at 250 and 273 K were fit with a two-exponential decay. Data taken at 294 K were fit with a single-exponential decay. (B) Plot of the decays of the Q_A^-Fe EPR signal versus dark incubation time at (●) 250 K and (△) 273 K. The Q_A^-Fe EPR signal was produced by illumination at 200 K after the S3 EPR signal had been induced. Data taken at 250 K were fit with a two-exponential decay. Data taken at 273 K were fit with a single-exponential decay.

temperatures. On the other hand, the rate of oxidation of a donor-side species increases as the illumination temperature is increased. The rates of formation and decay of the S3 and Q_A^-Fe EPR signals in acetate/PPBQ-treated PSII have been measured as a function of temperature. These results are summarized in Figures 4 and 5. Figure 4 shows the yield of the S3 EPR signal as a function of illumination time at three temperatures. At 250 K, the S3 EPR signal yield increased as a function of illumination time to reach a steady-state value of approximately 15%. At 0 °C and room temperature, the S3 EPR signal yield was highest at the initial illumination times of 15 and 5 s, respectively. At 0 °C, the steady-state yield of the S3 EPR signal was also about 15−20%. The room temperature yield of the S3 EPR signal also decreases as a function of illumination time, although the samples were not subjected to long illumination times at this

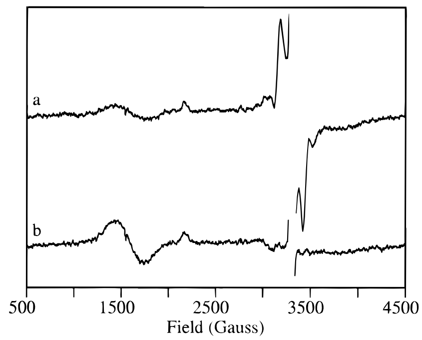

FIGURE 6: Light-minus-dark difference spectra of (a) the S3 EPR signal produced after 30 s of continuous illumination at 0 °C and (b) the same sample after dark incubation at 250 K for 1.25 h. [Chl] = 6 mg/mL.

temperature in order to avoid possible photodamage of the sample.

The results of these experiments support our conclusion that an acceptor-side source of the S3 EPR signal can be ruled out. Because oxidation of Q_A^- is faster at higher temperatures, if the S3 EPR signal were due to an acceptor-side species, such as Q_A^- interacting with the non-heme iron, we would expect the yield of the S3 EPR signal to decrease as the illumination temperature was increased. In fact, the reverse trend was observed. It may be, then, that the S3 EPR signal yield directly depends on the rate of an acceptor-side reaction.

In order to determine whether S-state advancement is involved in the pathway of S3 EPR signal formation, we monitored the S3 EPR signal decay and found that the $g = 4.1$ EPR signal due to the S_2 state of the OEC was observed as an intermediate in the decay (Figure 6). The $g = 4.1$ form of the S_2 state has previously been observed in acetate- and FCCP-treated PSII (MacLachlan & Nugent, 1993). Because FCCP mediates nonspecific redox processes in PSII (Ghanotakis et al., 1982; Packham & Barber, 1984; Packham & Ford, 1986), an observation of the S_2-state $g = 4.1$ EPR signal in acetate- and FCCP-treated PSII does not address the question of whether the S_2 state is on the path to formation of the S3 EPR signal. Figure 7A shows that at 0 °C the rate of decay of the S3 EPR signal matches the rate of formation of the $g = 4.1$ S_2-state EPR signal. The same is true of the data collected at room temperature (Figure 7B). Together with the flash results, formation of the S_2 state upon decay of the S3 EPR signal supports a two-step process as shown in eq 1:

$$\underset{\text{dark}}{S_1X} \underset{k_2}{\overset{h\nu}{\rightleftharpoons}} \underset{g=4.1}{S_2X} \underset{k_1}{\overset{h\nu}{\rightleftharpoons}} \underset{\text{broad radical}}{S_2X^+} \qquad (1)$$

The S3 EPR signal has been attributed to an organic radical species that is weakly interacting with the S_2 state of the OEC. If this is correct, it is unclear why an EPR signal arising from the S_2 state is not observable under conditions that produce the S3 EPR signal in acetate-treated PSII. The explanation that has been used is that the S_2 state interacting with the organic radical gives rise to a broadened multiline S_2-state EPR signal that does not exhibit well-resolved hyperfine structure (Boussac et al., 1989, 1990b; Baumgarten et al., 1990; MacLachlan & Nugent, 1993). However, in the case of acetate-treated PSII, the S_2-state $g = 4.1$ EPR signal should be observable, even if somewhat broadened

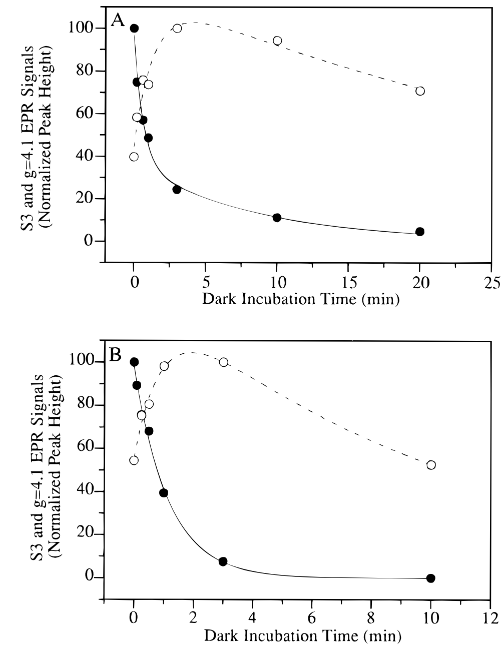

FIGURE 7: Plots of the decay of the S3 EPR signal (●) and formation of the S_2-state $g = 4.1$ EPR signal (○) as a function of dark incubation time. The S3 EPR signal decays were fit as described in the legend of Figure 5. The formation of the S_2-state $g = 4.1$ EPR signal was fit with the equation: intensity $= Ae^{-k_1t} - Be^{-k_2t}$. (A) Dark incubation at 273 K. (B) Dark incubation at 294 K.

by a weak interaction with an organic radical. One possible explanation of the apparent suppression of the S_2-state $g = 4.1$ EPR signal when the S3 EPR signal is present (Figures 6 and 7) is that the $g = 4.1$ and S3 EPR signals arise from different PSII centers. However, our observation that the rate of formation of the $g = 4.1$ EPR signal matches the rate of decay of the S3 EPR signal at both 273 K and 294 K argues against this possibility. Alternatively, the lack of an EPR signal at $g = 4.1$ when the S3 EPR signal is present may be explained if the effect on the Mn_4 cluster by the organic radical is larger than has been previously thought. In this case, the overall spin state of the Mn_4 cluster could change without a formal oxidation state change of the Mn_4 cluster such that the S_2 state produced in the presence of the organic radical does not exhibit an observable EPR signal. Decay of the oxidized organic species would eliminate the interaction and replace the EPR-silent S_2 state with the $g = 4.1$ form. The S3 EPR signal could still arise from an organic radical that is weakly exchange and/or dipolar coupled to the Mn_4 cluster, but the structure of the Mn_4 cluster would be more sensitive to the oxidation state of the organic radical than previously thought. In support of this possibility is the observation that the S_2-state multiline EPR signal is altered by calcium depletion or acetate treatment, even when there is no S3 EPR signal present. The changes in the S_2-state EPR signals have been ascribed to changes in the environment surrounding the Mn_4 cluster caused by the treatments (Boussac et al., 1989; Ono & Inoue, 1990; Andréasson & Lindberg, 1992; Van Vliet et al., 1994).

Kinetics. The data on the S3 EPR signal yield as a function of illumination time and temperature provide evidence that the yield of the S3 EPR signal is not determined exclusively by reactions associated with its formation, but also by decay reactions. To develop a kinetic model to account for the yield of the S3 EPR signal as a function of

Table 2: Rate Constants and Amplitudes of Decays of the S3 and Q_A^-Fe EPR Signals at Different Temperatures in Acetate-Treated PSII

	S3 EPR signal decay		Q_A^- EPR signal decay	
T (K)	k_{S3}(fast) (min^{-1}) (amplitude, %)	k_{S3}(slow) (min^{-1}) (amplitude, %)	k_{QA}(fast) (min^{-1}) (amplitude, %)	k_{QA}(slow) (min^{-1}) (amplitude, %)
250	1.04 ± 0.23 (46 ± 4)	0.012 ± 0.003 (56 ± 3)	0.18 ± 0.05 (38 ± 13)	0.028 ± 0.009 (62 ± 14)
273	1.55 ± 0.45 (61 ± 10)	0.12 ± 0.05 (36 ± 10)	5.67 ± 0.62 (99 ± 4)	
294		0.87 ± 0.06 (98 ± 2)		

illumination time and temperature, the rates of decay of both the S3 and Q_A^-Fe EPR signals were measured. The results of these experiments are shown in Figure 5A,B, and the rate constants are summarized in eq 2 and Table 2. At 250 K, the decays of both the S3 and Q_A^-Fe EPR signals were biphasic, whereas the decays were monophasic at the higher temperatures. However, the rate of Q_A^- oxidation was not similar to the rate of decay of the S3 EPR signal at any of the temperatures examined; therefore, our measured decays cannot be ascribed to recombination of the S3 EPR signal species with Q_A^-. The decay of the S3 EPR signal could be attributed to reduction of the S3 EPR signal species by an external reductant, probably reduced PPBQ. The decay of the Q_A^-Fe EPR signal could be due to oxidation of Q_A^- by PPBQ. It is likely that the slower phases for decay observed at 250 K are due to heterogeneity of the samples. For example, the Q_B site is expected to be only partially occupied by PPBQ, and centers with an empty Q_B site would have slower Q_A^- oxidation owing to slow diffusion at 250 K.

At 0 °C, the S3 EPR signal decay was still biphasic, but the amplitude of the faster phase increased. Boussac et al. (1989) observed a monophasic decay of the S3 EPR signal at 0 °C in calcium-depleted PSII ($t_{1/2} \approx 4.5$ min which corresponds to $k = 0.15$ min^{-1}). This rate constant is similar to the slower phase of S3 EPR signal decay at 0 °C in our samples. Deconvolution of the S3 EPR signal decay into two components relies on the use of short incubation times. The incubation times used by Boussac et al. (1989) may not have been short enough to observe a fast phase in the decay of the S3 EPR signal.

At 0 °C and at room temperature, the Q_A^-Fe EPR signal decay was monophasic. As the temperature is raised, electron transfer from Q_A^- to PPBQ becomes faster owing to faster diffusion of PPBQ to/from the Q_B site. This could explain why the decay of the Q_A^-Fe EPR signal at 0 °C occurs faster than the decay of the S3 EPR signal. At room temperature, the S3 EPR signal decay also was monophasic, probably because the fast phase found at 250 K and 0 °C was unobservable at higher temperatures. Additionally, no Q_A^-Fe EPR signal was observed in these samples because the rate of oxidation of Q_A^- was too fast at this temperature.

The rate constants from the decay data and the temperature dependence of the S3 EPR signal yield have been used to generate a kinetic model that accounts for the observed steady-state yields of the S3 EPR signal. Equation 2a shows the photochemical steps leading to the formation of the S3 EPR signal. A two-step photochemical process is used based on the flash experiments showing that only two turnovers are required to form the S3 EPR signal. The first charge separation will generate the state $S_2XQ_A^-$ which must bind a quinone molecule to form the state $S_2XQ_AQ_B^-$. The binding of quinone is expected to be slow, especially at lower temperatures. However, once the state $S_2XQ_AQ_B^-$ has been formed, the second turnover will be rapid and will yield the S3 EPR signal species. In our studies of the decay of the Q_A^-Fe EPR signal (Figure 5), the sample was illuminated at 200 K after the S3 EPR signal had been induced in order to photoreduce Q_A. (At 200 K, cytochrome b_{559} or a chlorophyll species, referred to as Chl_Z, functions as the electron donor.) The decay reactions and the associated rate constants are shown in eq 2b.

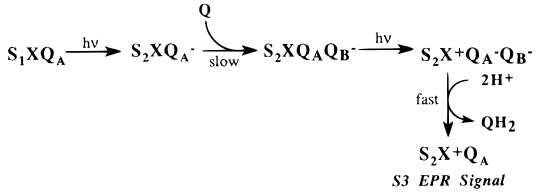

(2a)

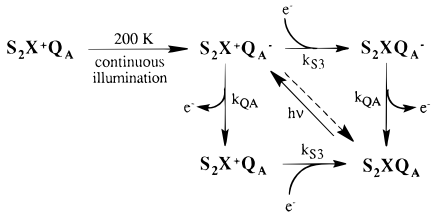

(2b)

In the kinetic model, it was assumed that the first charge separation to generate the state $S_2XQ_A^-$ is much faster than all of the other steps. Based on the observation that the S3 and Q_A^-Fe EPR signals decay at different rates, the model includes independent decay pathways for the two species. As already mentioned, the major phases for decay of Q_A^- and the S3 EPR signal species could be oxidation by PPBQ and reduction by an external reductant, respectively. By using the measured rate constants for the fast phases of decay of the S3 EPR signal species and oxidation of Q_A^- (Table 2), we can model the yield and rate of formation of the S3 EPR signal at 250 K. The result of this calculation is shown by the solid line in Figure 4. The yield of the S3 EPR signal at 250 K is small because both Q_A^- oxidation and S-state advancement are slow at this temperature and alternate donors such as cytochrome b_{559} are preferentially oxidized in most centers. Since the charge-separated state cytochrome b_{559}^{ox}/Q_A^- is relatively stable, further turnover to produce the S3 EPR signal requires oxidation of Q_A^-.

As the temperature is increased, two key observations are that the maximal yield of the S3 EPR signal increases and that the maximal yield is induced at shorter illumination times. Both of these obserations are explained if the yield of the S3 EPR signal is determined by the rate of Q_A^- oxidation. However, in contrast to the 250 K data, the yields and rates of formation of the S3 EPR signal observed at

higher temperatures cannot be modeled well with eq 2. The model predicts that, at higher temperatures, the yield of the S3 EPR signal should initially be high and remain high at longer illumination times. In contrast, the yield of the S3 EPR signal drops as the illumination time increases. One explanation for this result is that, as the system turns over, the quinone pool becomes increasingly reduced. If the yield of the S3 EPR signal is determined by the rate of Q_A^- oxidation, the yield of the S3 EPR signal will decrease as the concentration of reduced PPBQ increases. However, O_2 evolution is inhibited in acetate-treated PSII, and, therefore, it is not expected that the PPBQ pool would become significantly reduced. Alternately, the decrease in S3 EPR signal yield at higher temperatures could be the result of photodamage. Indeed, we find that acetate-treated PSII samples lose 40% of the O_2 evolution activity after 10 min of illumination at room temperature under the illumination conditions used for the EPR samples. Inhibited PSII samples are especially sensitive to photodamage, and Y_Z has been found to be the initial site of photodamage under continuous illumination (Chen et al., 1995). If $Y_Z^\bullet$ is the source of the S3 EPR signal as has been proposed (Hallahan et al., 1992; Gilchrist et al., 1995), photodamage would decrease the S3 EPR signal yield as a function of illumination time. This could explain why the yields of the S3 EPR signal at 273 K and 294 K are highest at the shortest illumination times used.

CONCLUSIONS

By using fully oxidized $Y_D^\bullet$ as an internal spin standard and optimizing illumination conditions, the maximum percentage of centers giving rise to the S3 EPR signal was found to be 49 ± 3%. Even with the optimal conditions, about half of the centers in acetate-treated PSII still do not produce an S3 EPR signal. The yield of the S3 EPR signal is shown to be determined by competing formation and decay reactions. Further increases in the yield of the S3 EPR signal may be possible by using a better electron acceptor such as a redox-active herbicide (Bocarsly & Brudvig, 1992) that can accept electrons from Q_A^- at lower temperatures where decay of the S3 EPR signal species is minimized and photodamage to the sample is reduced.

ACKNOWLEDGMENT

We thank David Stewart for his assistance in performing the saturating laser-flash experiments.

REFERENCES

Andréasson, L.-E., & Lindberg, K. (1992) *Biochim. Biophys. Acta 1100*, 177−183.
Arnon, D. I. (1949) *Plant Physiol. 24*, 1−15.
Baumgarten, M., Philo, J. S., & Dismukes, G. C. (1990) *Biochemistry 29*, 10814−10822.
Beck, W. F., de Paula, J. C., & Brudvig, G. W. (1985) *Biochemistry 24*, 3035−3043.
Berthold, D. A., Babcock, G. T., & Yocum, C. F. (1981) *FEBS Lett. 134*, 231−234.
Blubaugh, D., & Govindjee (1988) *Photosynth. Res. 19*, 85−128.
Bocarsly, J. R., & Brudvig, G. W. (1992) *J. Am. Chem. Soc. 114*, 9762−9767.
Boussac, A., & Rutherford, A. W. (1988) *Biochemistry 27*, 3476−3483.
Boussac, A., & Rutherford, A. W. (1992) *Biochemistry 31*, 7441−7445.
Boussac, A., Zimmermann, J.-L., & Rutherford, A. W. (1989) *Biochemistry 28*, 8984−8989.
Boussac, A., Zimmermann, J.-L., & Rutherford, A. W. (1990a) *FEBS Lett. 277*, 69−74.
Boussac, A., Zimmermann, J.-L., Rutherford, A. W., & Lavergne, J. (1990b) *Nature 347*, 303−306.
Boussac, A., Setif, P., & Rutherford, A. W. (1992) *Biochemistry 31*, 1224−1234.
Brudvig, G. W., Casey, J. L., & Sauer, K. (1983) *Biochim. Biophys. Acta 723*, 366−371.
Buser, C. A., & Brudvig, G. W. (1992) in *Current Research in Photosynthesis* (Murata, N., Ed.) pp 85−88, Kluwer Academic Publishers, Dordrecht, The Netherlands.
Chen, G. X., Blubaugh, D. J., Homann, P. H., Golbeck, J. H., & Cheniae, G. M. (1995) *Biochemistry 34*, 2317−2332.
Damoder, R., Klimov, V. V., & Dismukes, G. C. (1986) *Biochim. Biophys. Acta 848*, 378−391.
Debus, R. J. (1992) *Biochim. Biophys. Acta 1102*, 269−352.
Dekker, J. P., van Gorkom, H. J., Wensink, J., & Ouwehand, L. (1984) *Biochim. Biophys. Acta 767*, 1−9.
dePaula, J. C., Beck, W. F., Miller, A.-F., Wilson, R. B., & Brudvig, G. W. (1987) *J. Chem. Soc., Faraday Trans. 1 83*, 3635−3651.
Dismukes, G. C., & Siderer, Y. (1980) *FEBS Lett. 121*, 78−80.
Ghanotakis, D. F., & Yocum, C. F. (1990) *Annu. Rev. Plant Physiol. Plant Mol. Biol. 41*, 255−276.
Ghanotakis, D. F., Yerkes, C. T., & Babcock, G. T. (1982) *Biochim. Biophys. Acta 682*, 21−31.
Gilchrist, M. L., Lorigan, G. A., & Britt, R. D. (1992) in *Current Research in Photosynthesis* (Murata, N., Ed.) pp 317−320, Kluwer Academic Publishers, Dordrecht, The Netherlands.
Gilchrist, M. L., Jr., Ball, J. A., Randall, D. W., & Britt, R. D. (1995) *Proc. Natl. Acad. Sci. U.S.A. 92*, 9545−9549.
Guiles, R. D., Zimmermann, J.-L., McDermott, A. E., Yachandra, V. K., Cole, J. L., Dexheimer, S. L., Britt, R. D., Wieghardt, K., Bossek, U., Sauer, K., & Klein, M. P. (1990) *Biochemistry 29*, 471−485.
Haddy, A., Dunham, W. R., Sands, R. H., & Aasa, R. (1992) *Biochim. Biophys. Acta 1099*, 25−34.
Hallahan, B. J., Nugent, J. H. A., Warden, J. T., & Evans, M. C. W. (1992) *Biochemistry 31*, 4562−4573.
Itoh, S., Yerkes, C. T., Koike, H., Robinson, H. H., & Crofts, A. R. (1984) *Biochim. Biophys. Acta 766*, 612−622.
Kok, B., Forbush, B., & McGloin, M. (1970) *Photochem. Photobiol. 11*, 457.
Koulougliotis, D., Hirsh, D. J., & Brudvig, G. W. (1992) *J. Am. Chem. Soc. 114*, 8322−8323.
MacLachlan, D. J., & Nugent, J. H. A. (1993) *Biochemistry 32*, 9772−9780.
MacLachlan, D. J., Nugent, J. H. A., Warden, J. T., & Evans, M. C. W. (1994) *Biochim. Biophys. Acta 1188*, 325−334.
Nugent, J. H. A., MacLachlan, D. J., Rigby, S. E. J., & Evans, M. C. W. (1993) *Photosynth. Res. 38*, 341−346.
Ono, T., & Inoue, Y. (1990) in *Current Research in Photosynthesis* (Baltscheffsky, M., Ed.) pp 741−744, Kluwer Academic Publishers, Dordrecht, The Netherlands.
Ono, T., Noguchi, T., Inoue, Y., Kusunoki, M., Matsushita, T., & Oyanagi, H. (1992) *Science 258*, 1335−1337.
Ono, T., Noguchi, T., Inoue, Y., Kusunoki, M., Yamaguchi, H., & Oyanagi, H. (1994) *Biochem. Soc. Trans. 22*, 331−335.
Packham, N. K., & Barber, J. (1984) *Biochem. J. 221*, 513−520.
Packham, N. K., & Ford, R. C. (1986) *Biochim. Biophys. Acta 852*, 183−190.
Rutherford, A. W., Zimmermann, J.-L., & Boussac, A. (1992) in *The Photosystems: Structure, Function, and Molecular Biology* (Barber, J., Ed.) pp 179−229, Elsevier Science Publishers, Amsterdam.
Saygin, Ö., Gerken, S., Meyer, B., & Witt, H. T. (1986) *Photosynth. Res. 9*, 71−78.
Sinclair, J. (1984) *Biochim. Biophys. Acta 764*, 247−252.
Sivaraja, M., Tso, J., & Dismukes, G. C. (1989) *Biochemistry 28*, 9459−9464.
Szalai, V. A., & Brudvig, G. W. (1995) *Biophys. J. 68*, A92.
Theg, S. M., Jursinic, P. A., & Homann, P. H. (1984) *Biochim. Biophys. Acta 766*, 636−646.
Van Vliet, P., Boussac, A., & Rutherford, A. W. (1994) *Biochemistry 33*, 12998−13004.

BI952378T